Analysis of systematic errors in lateral shearing interferometry for EUV optical testing

Ryan Miyakawa[a,b], Patrick Naulleau[b], and Ken Goldberg[b]

[a]Applied Science & Technology Graduate Group, University of California, Berkeley
Berkeley, CA 94720, USA
[b]Center for X-ray Optics, Lawrence Berkeley National Laboratory
1 Cyclotron Road, Berkeley, CA 94720, USA

ABSTRACT

Lateral shearing interferometry (LSI) provides a simple means for characterizing the aberrations in optical systems at EUV wavelengths. In LSI, the test wavefront is incident on a low-frequency grating which causes the resulting diffracted orders to interfere on the CCD. Due to its simple experimental setup and high photon efficiency, LSI is an attractive alternative to point diffraction interferometry and other methods that require spatially filtering the wavefront through small pinholes which notoriously suffer from low contrast fringes and improper alignment. In order to demonstrate that LSI can be accurate and robust enough to meet industry standards, analytic models are presented to study the effects of unwanted grating and detector tilt on the system aberrations, and a method for identifying and correcting for these errors in alignment is proposed. The models are subsequently verified by numerical simulation. Finally, an analysis is performed of how errors in the identification and correction of grating and detector misalignment propagate to errors in fringe analysis.

Keywords: shearing interferometry, grating, aberrations, optical testing

1. INTRODUCTION

Due to increasing demands for higher resolution optical systems for EUV lithography, it is becoming more important to have a simple and reliable procedure for characterizing the aberrations present in the optics. Conventional point diffraction interferometry that interferes the test wavefront with a spherical reference wave generated by a pinhole becomes increasingly difficult at higher numerical apertures since the size of the pinhole is chosen to match the diffraction limit of the optical system which can be as small as 12 nm for next-generation EUV tools. In practice, small pinholes are cumbersome because they are difficult to locate, they clog up easily, and the low photon flux that exits the pinhole makes for poor contrast in the interferogram.[1]

Shearing interferometry eliminates the need for a high quality reference wave by interfering the test wavefront with a shifted (sheared) copy of itself. The reconstructed phasemap is thus an approximation to the derivative of the test wavefront in the direction of the shear:

$$U(x,y) = W(x+s,y) - W(x,y) \approx s\frac{dW(x,y)}{dx} \tag{1}$$

and can be reconstructed using numerical methods.[2]

In visible light shearing interferometry a beamsplitter can be used to shear the test wavefront. At EUV wavelengths, however, a diffraction grating must be used. Special care must be taken when using diffraction gratings because a wavefront will not in general preserve its shape as it is diffracted by a grating. It is therefore necessary to decouple the aberrations created by the grating from the aberrations in the optic itself. Grating aberrations are highly sensitive to grating and detector tilt, which means that it is critical that the LSI setup is properly aligned. From an analytic model it can be shown that the grating and detector tilt can be extracted

Further author information: (Send correspondence to Ryan Miyakawa)
E-mail: rhmiyakawa@lbl.gov

from experimental data that is independent of aberrations in the optical system, which can be used to align the experiment. Finally, it will be seen that grating tilt aberrations form a basis of Zernike polynomials that do not represent valid outputs of the LSI system, which can be used to monitor the status of the alignment of the system, should the grating drift from proper alignment.

2. SYSTEMATIC ABERRATIONS DUE TO GRATING DISTORTION

Since aberrations in an optical system are measured as deviations of the wavefront from a sphere, it is important to examine the aberrations that arise from performing diffraction based LSI on an un-aberrated spherical wave.

When a plane wave is incident on a diffraction grating at an angle θ_i, its n-th order diffraction angle θ_f is given by the grating equation:

$$\frac{\sin\theta_f}{\lambda} = \frac{\sin\theta_i}{\lambda} + \frac{n}{T} \tag{2}$$

where T is the period of the grating. Since θ_f and θ_i are not linearly related, diffracted plane waves experience a different angular shift $\Delta\theta$ depending on their incident angle. As a consequence, diffracted wavefronts do not, in general, preserve their shape. In particular, the diffracted spherical wave in the LSI setup gains significant aberrations which invalidates the approximation in (1). It is therefore necessary to know these aberrations a priori and subtract them from the experimental data in the analysis.

A simple model can be used to solve for the grating aberrations analytically. In this model, a grating with two diffraction orders,

$$t_g(x,y) = 1 + \exp\left(2\pi i x/T\right) \tag{3}$$

is constructed holographically by interfering a spherical reference wave and an unknown object beam that originates at a virtual source point that is displaced by an angle of θ_f. Due to the uniqueness of the hologram, this scenario is equivalent to diffracting a single spherical wave off of the grating in (3). The additional phase function $k\Phi(x,y)$ added to the diffracted sphere can then be solved in closed form, and is given by:

$$k[r(x+d,y) + \Phi(x,y)] = 2\pi x/T \tag{4}$$

where $k = 2\pi/\lambda$. After some simplification and standard interferogram analysis, and converting Φ to polynomial form, the aberrations present in the null interferogram are revealed as:

$$\begin{aligned} W_{0,1}(\rho,\theta) = &\left(\frac{\xi}{T} + \frac{d^2}{2\xi T}\right) NAZ_1(\rho,\theta) \\ &- \left(\frac{d}{2T}\right) NA^2 Z_3(\rho,\theta) - \left(\frac{d}{4T}\right) NA^2 Z_4(\rho,\theta) \end{aligned} \tag{5}$$

where Z_i represents the ith Zernike fringe coefficient and NA is the numerical aperture of the system. The resulting phase contains quadratic error terms in the form of astigmatism and defocus which are present in the null interferogram. Failure to account for these systematic errors would result in cubic terms such as coma in the reconstructed wavefront. In the next section it will be shown that these systematic errors are highly dependent on the alignment of the LSI experiment which ultimately sets a lower bound on the accuracy of LSI.

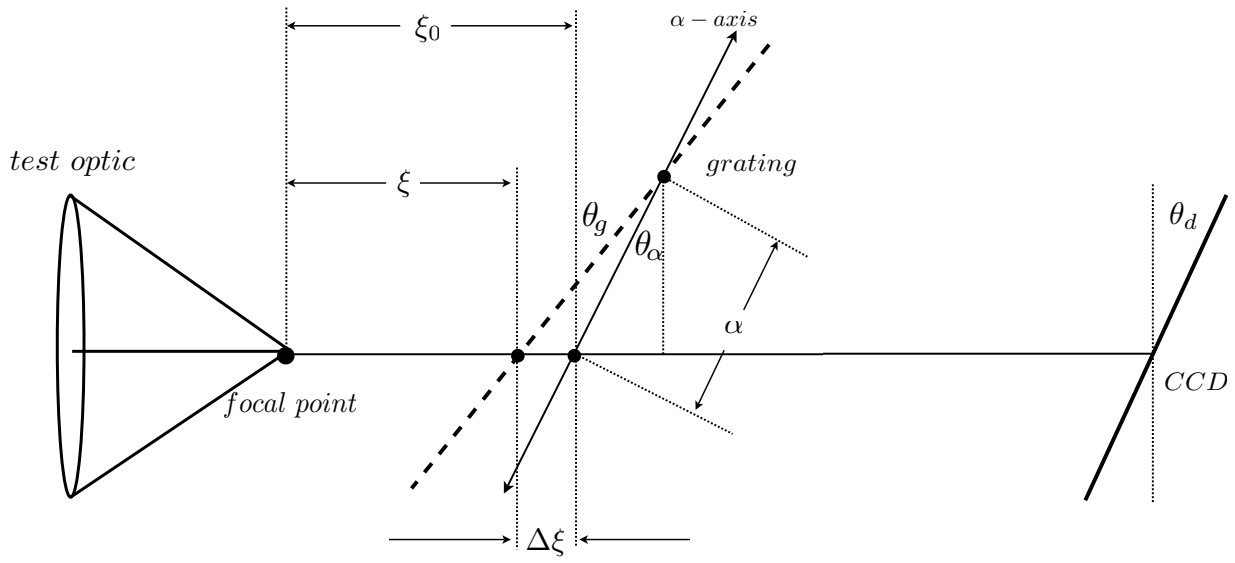

Figure 1. Geometry of the LSI experimental setup. Tilt angles θ_g and θ_d are exaggerated for clarity

3. EFFECTS OF TILT ON SYSTEMATIC ABERRATIONS

In this section, an analytical model is presented that determines the relationship between systematic aberrations and the system alignment, and a method is proposed to determine and correct for these alignment errors. For clarity, the analysis is presented in 1D, although the extension to 2D is relatively straightforward.

The geometry of the experiment is shown in Figure 1. The grating and the detector to be out of alignment by the angles θ_g and θ_d respectively, measured from the planes orthogonal to the optical axis; The grating rotation stage has an axis which is offset from the optical axis by an amount α, measured along the axis of grating translation; θ_α represents the angular displacement of the axis of grating translation to the plane perpendicular to the optical axis; ξ represents the distance between the focal plane of the test optic and the grating along the optical axis.

In the previous section, an expression for the 1-D wavefront phase-map was effectively determined at any arbitrary coordinate (x, z). A simple way to deal with the grating and detector tilts is to perform a coordinate transformation that aligns the z-axis perpendicular to the grating, and reparameterize the optical axis coordinate and the detector coordinate in terms of this new z. Mathematically, this is represented as the following transformation:

$$\begin{bmatrix} x \\ z \end{bmatrix} = \begin{bmatrix} \cos(\theta_g - \theta_d) & \sin(\theta_g) \\ -\sin(\theta_g - \theta_d) & \cos(\theta_g) \end{bmatrix} \cdot \begin{bmatrix} \chi \\ \zeta \end{bmatrix} \tag{6}$$

The parameter ξ which measures the distance between the focus of the optic and the grating along the optical axis, must also be modified to account for the grating tilt and the coordinate transformation.

$$\begin{aligned} \xi &= (\xi_0 - \Delta\xi)\cos\theta_g \\ &= \xi_0 \cos\theta_g - \alpha(\cos\theta_\alpha \sin\theta_g - \sin\theta_\alpha \cos\theta_g) \end{aligned} \tag{7}$$

Applying these transformations to the result in (5) allows one to write out the aberrations explicitly as a function of the alignment parameters.

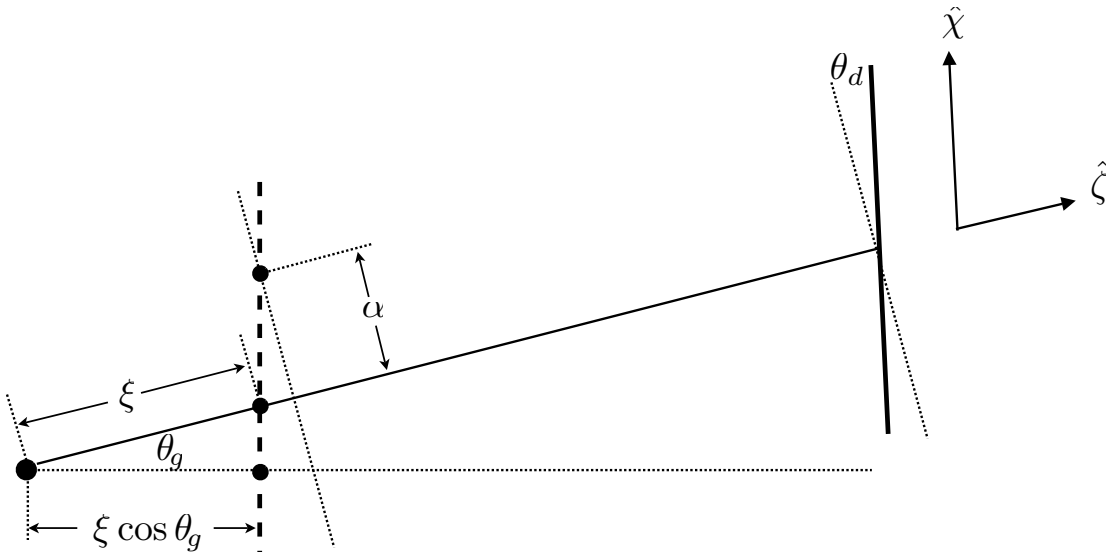

Figure 2. Geometry in rotated coordinate system

$$\begin{aligned} a_1 &= f(\theta_g, \theta_d, \theta_\alpha, \alpha) \\ a_2 &= g(\theta_g, \theta_d, \theta_\alpha, \alpha) \\ &\vdots \end{aligned} \tag{8}$$

Figure 3 shows simulation results plotted against the analytical forms above, which are in good agreement. The following procedure outlines the method for using experimental data to solve for the unknown alignment parameters:

1. Align the CCD detector to be perpendicular to the optical axis by finding the θ_d that maximizes the fringe density on the detector.
2. Collect interferograms for many ($\sim$30) different grating tilt angles and measure the resulting tilt and astigmatism in the fringes for two distinct grating translations.
3. Align grating to the tilt of its translation stage axis by noting that aberrations will be independent of grating displacement at this tilt angle.
4. Perform a polynomial fit of the linear and quadratic terms as a function of grating tilt angle using the translation stage tilt as the origin
5. Match the resulting terms of the fit to their analytic model depending on the slope of the model around the recovered angle

Because the alignment procedure relies on the trends of the aberration data rather than the values of the aberrations themselves, it works even in the presence of intrinsic aberrations in the optical system provided that they are small in magnitude compared to the base carrier sphere. Numerical simulations implementing the above alignment procedure under reasonable experimental conditions show that the LSI system can be aligned to within $\lambda_{EUV}/100$ of rms wavefront error.

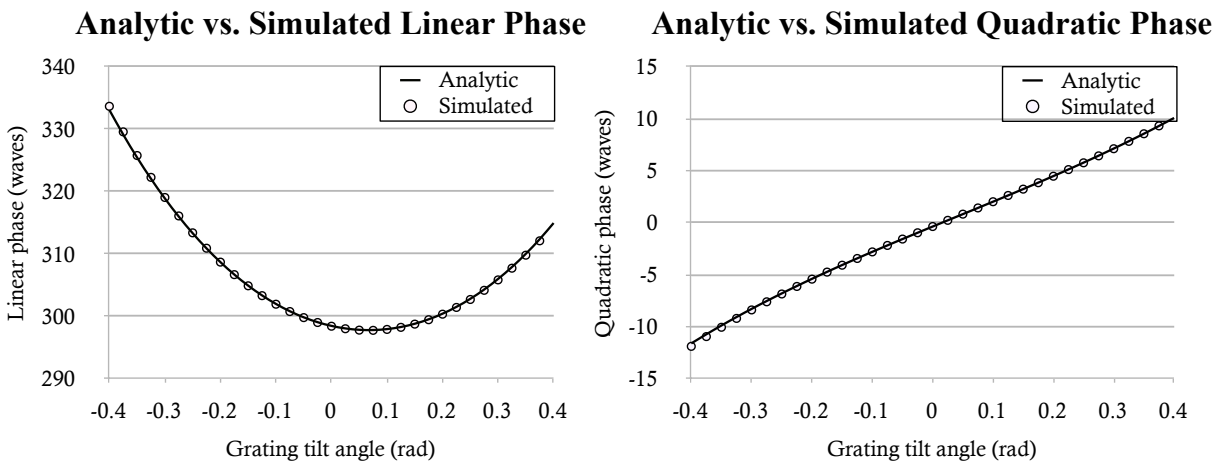

Figure 3. Analytic forms for systematic linear and quadratic phase with overlay of simulated results. The plots reflect $\lambda = 13.4\ nm$, $z_1 = 2606.52\ \mu m$, $NA = .08$, $\theta_\alpha = \theta_d = 0$, and $\alpha = 0$

4. MONITORING THE HEALTH OF THE SYSTEM

The aberrations present in the LSI interferogram are not the aberrations in the optical system itself; rather, they measure the x- and y-derivatives of the test wavefront. In this sense, the LSI setup can be thought of as a linear system D that maps the space of wavefronts of N Zernike polynomials W_N to its x- and y-derivatives. Let $V_{N\times N}$ be the space of the x- and y- derivatives of Zernike polynomials of order N or less. Then we can define the operation of D as:

$$\begin{aligned} D : W_N &\longmapsto V_{N\times N} \\ D(w) &= [\partial_x(w), \partial_y(w)] \end{aligned} \tag{9}$$

Since the domain W_N has dimension N and the codomain $V_{N\times N}$ has dimension $2N$, D is not surjective. In other words, there is set $\mathscr{F} = \{V_{N\times N}\} \setminus \{D(W)\}$ of *forbidden* solutions, which are a basis of x- and y-derivatives that cannot come from a valid wavefront.

As an illustration, consider the x-derivative $\partial_x W(x,y) = y$. This would imply that the original wavefront $W(x,y) = xy$, which means that there should be a y-derivative $\partial_y W(x,y) = x$. Thus, it is clear that $[\partial_x W(x,y), \partial_y W(x,y)] = [y, 0]$ belongs to $\mathscr{F}$.

In general the dimension of $\mathscr{F}$ is N, and although it will not be proved here, the following relation holds

$$W_N \times W_N = \{D(W)\} \oplus \mathscr{F} \tag{10}$$

where $\oplus$ denotes a direct sum, meaning that every vector $\vec{v} \in V_{N\times N}$ is either in $\mathscr{F}$ or in $D(W)$. To apply this result we project the shearing interferogram into $D(W)$ and $\mathscr{F}$. A valid interferogram should have 100% projection into $D(W)$ and 0% projection into $\mathscr{F}$. To be precise, if β is a basis for $D(W)$, γ is a basis for $\mathscr{F}$, and $\vec{w} \in V_{N\times N}$ is the wavefront derivatives vector, then the ratio:

$$R = \frac{\sum_{k=1}^{N} |\beta_k \cdot w|^2}{\sum_{k=1}^{N} |\beta_k \cdot w|^2 + \sum_{k=1}^{N} |\gamma \cdot w|^2} \tag{11}$$

which is the fractional projection of $\vec{w}$ on $D(W)$ can be seen as a measure of the health of the LSI system. In a properly aligned system, $R = 1$. When $R < 1$, the system has drifted from alignment, which causes invalid aberrations measured in the interferogram.

5. LIMITATIONS OF DIFFRACTION-BASED LSI

Because the systematic aberrations in LSI are highly sensitive to system alignment, the accuracy of the optical characterization is ultimately set by the ability to remove these systematic aberrations in the analysis. While a rigorous error analysis will not be presented here, it should be pointed out that there are a number of factors can limit the accuracy of the alignment process.

5.1. Requirement of detector stage

A critical step in the system alignment is aligning the detector to be perpendicular to the optical axis ($\theta_d \rightarrow 0$). Even tilt angles of a few milliradians will generate large quadratic phase terms. Nevertheless, the detector can be aligned with extreme accuracy ($\sigma_{\theta_d} \approx 10^{-6}$ rad) by sweeping θ_d and tracking the fringe density. It is therefore required to have the ability to tilt the detector about both x- and y-axes.

5.2. Uncertainty in grating rotation stage

Because the alignment procedure relies heavily on the relationship between the measured phase terms and the grating tilt, it is imperative that the grating tilt stage be stable and precise. The accuracy of the optical characterization scales linearly with grating tilt stage precision, and to achieve a wavefront accuracy of $\lambda_{EUV}/100$ the grating tilt must be known to within $\sigma_{\theta_g} = 50\ \mu rad$.

5.3. Grating translation parallelism

Phase measurements are also highly sensitive to the location of the grating along the optical axis. Therefore, the grating must not wiggle appreciably from side to side in the z-direction as it is translated in the x- and y-directions. To ensure a wavefront accuracy of $\lambda_{EUV}/100$, the grating translation stage rms deviation must be less than 50 nm.

5.4. Requirement of large data-set

The alignment procedure requires a minimum of 60 interferograms to be taken, although more is be better since the accuracy of the alignment increases with number of exposures. Collecting such a large number of data points can take a long time depending on the photon throughput of the system, and it is important that the system alignment does not drift from exposure to exposure.

6. CONCLUSION

LSI is an attractive method for characterizing aberrations in future EUV systems due to its simple setup and its ability to scale to high numerical apertures. Performing LSI via diffraction-based shear introduces significant systematic aberrations that must be removed from the data in the analysis. These aberrations are further exacerbated by grating and detector tilt, and the LSI setup must therefore be properly calibrated before the experiment is done. Although LSI requires high precision translation and rotation stages to combat the high sensitivity of the system to misalignment, and the ability for the system to remain static over the period in which the interferograms are taken, it remains a leading candidate among metrologies for next-generation EUV tools.

ACKNOWLEDGMENTS

The authors are grateful for support from the NSF EUV Engineering Research Center. Lawrence Berkeley National Laboratory is operated under the auspices of the Director, Office of Science, Office of Basic Energy Science, of the US Department of Energy. Work supported under Contract No. DE-AC02-05CH11231.

REFERENCES

1. P. P. Naulleau, K. A. Goldberg, et al., Applied Optics 38 (35), 7252-63 (1999), "Extreme-ultraviolet phase-shifting point-diffraction interferometer: a wave-front metrology tool with subangstrom reference-wave accuracy"
2. M. P. Rimmer, Applied Optics Vol. 13, No. 3, March 1974, "Method for Evaluating Lateral Shearing Interferograms"